DOI: https://doi.org/10.37434/tpwj2025.08.04

ELECTRODYNAMIC TREATMENT FOR THE CONTROL OF RESIDUAL STRESSES IN WELDED JOINTS MADE OF LIGHT, HEAT-RESISTANT ALLOYS AND AUSTENITIC STEEL

L.M. Lobanov, M.O. Pashchyn, O.L. Mikhodui, O.M. Tymoshenko

E.O. Paton Electric Welding Institute of the NASU
11 Kazymyr Malevych Str., 03150, Kyiv, Ukraine

ABSTRACT

The technology of electrodynamic treatment (EDT) of experimental specimens of thin-sheet butt welded joints made of Al-, Ni- and Ti-based alloys and austenitic steel was developed and implemented. Specialized assembly tooling was designed, which was used for automatic TIG welding of experimental specimens. The effect of EDT on the residual stress states of welded joint specimens was studied using the electron speckle interferometry method. It was found that EDT is an effective mechanism for the control of the residual stress states of welded joints made of Al and Ti alloys and austenitic steel. It is shown that in order to increase the effectiveness of EDT of Ni-based alloys, it is necessary to use higher values of electrodynamic effect power in further studies. It is also advisable to use a new treatment method based on magnetic pulsed effects on nonferromagnetic materials to optimize the residual stress states of welded joints made of Ni-based alloys.

KEYWORDS: Al-, Ni-, Ti-based alloys, austenitic steel, electrodynamic treatment, transport structures, welded joints, electron speckle interferometry, residual stress states, mechanical characteristics, chemical composition, treatment effectiveness, residual stress control

INTRODUCTION. RELEVANCE AND AIM OF THE STUDY

In the modern engineering practice of manufacturing thin-sheet welded transport structures, the traditional problem of extending their service life is associated with the need in optimizing the residual stress-strain states of welded joints. Tensile residual welding stresses (RWS) have a negative impact on the aero- and hydrodynamic characteristics, assembly accuracy, corrosion resistance and durability of products made of metal materials (MM), such as structural steels, aluminium, titanium, nickel-based alloys [1].

At present, new MM are used, which are an alternative to those traditionally used in the domestic production of transport structures. Thus, the problem of minimising the level of tensile RWS in welded joints made of new MM is relevant.

Electrophysical methods based on the use of pulsed electromagnetic fields of various lengths and configurations are challenging to control the stress states [2–12].

One of the electrophysical methods for the control of RWS is electrodynamic treatment (EDT) of welded joints, which proved its effectiveness in aircraft and shipbuilding [13–15]. The RWS relaxation during EDT occurs due to the electroplastic effect based on the synergy caused by the combined action of such components as pulsed current and dynamic load on the welded joint metal. The EDT, which can be used in manual and automatic modes, is adapted for the use in the process and after welding, including as part of automated (robotic) complexes [16, 17]. The EDT provides optimal positioning of the working tool — the electrode device (ED) — relative to the weld, the ability to treat welds of large structures in different spatial positions.

THE AIM OF THE STUDY

is to investigate the effectiveness of EDT application for the control of RWS in welded joints produced of MM, which are perspective for manufacturing of welded thin-sheet transport structures.

MECHANICAL CHARACTERISTICS OF MM

Four grades of MM were studied, which are used in the modern production of welded structures and belong to the class of "well-welded" ones. MM specimens were used in the form of sheets with overall dimensions of 500×200 mm and a thicknesses $\delta = 1.0$ and 3.0 mm. MM No. 1 is an Al-based alloy, further MM1 (Al). MM1 (Al) is used in the manufacture of shells, panels, fuel tanks, framework and saturation of transport hull structures. The chemical composition of MM1 (Al) is shown in Table 1.

MM No. 2 is a Ti-based alloy, further MM2 (Ti). MM2 (Ti) is used in the manufacture of framework, saturation, pipelines and hulls of transport structures.

Table 1. Chemical composition of MM1 (Al) alloy plates

Mg, %	Mn, %	Fe, %	Si, %	Al
2.29	0.3	0.2	0.11	Other

Table 2. Chemical composition of MM2 (Ti) titanium alloy plates

C, %	Si, %	Fe, %	N, %	H, %	O, %	Ti
0.0074	0.005	0.046	0.0079	0.0011	0.16	Other

Table 3. Chemical composition of high-temperature MM3 (Ni)alloy

C, %	S, %	P, %	Si, %	Mn, %	Cr, %	Ti, %	W, %	Fe, %	Al, %	Mo, %	Ni
0.055	0.0023	0.0019	0.13	0.28	24.44	0.43	14.37	0.075	0.25	0.75	Other

Table 4. Chemical composition of MM4 steel (Fe–Cr–Ni)

C, %	S, %	P, %	Si, %	Mn, %	Cr, %	Ni, %	Mo, %	W, %	Nb, %	V, %	Fe
0.069	0.0047	0.005	0.27	0.4	14.55	5.39	0.89	0.86	0.15	0.18	Other

Table 5. Basic mechanical characteristics of MM specimens δ = 1 and 3 mm

No.	Grade of MMs	δ, mm	Mechanical characteristics of MM		
			$\sigma_{0.2}$, MPa	σ_t, MPa	δ_y, %
1	MM1 (Al)	1.0	229.9/206.9	271.4	11.0/13.0
2		3.0	228.1	270.7	10.3
3	MM2 (Ti)	1.0	281.1	431.5	35.2
4		3.0	275.0	430.7	34.5
5	MM3 (Ni)	1.0	438.9	858.2	57.3
6		3.0	438.0	847.5	49.7
7	MM4 (Fe–Cr–Ni)	1.0	935.7	956.3	11.2
8		3.0	930.3	946.6	11.2

The chemical composition of MM2 (Ti) alloy is shown in Table 2.

MM No. 3 is a high-temperature Ni-based alloy, further MM3 (Ni). MM3 (Ni) is used for pipelines and load-bearing elements and parts of gas equipment operating at high temperatures. The chemical composition of MM3 (Ni) alloy is shown in Table 3.

MM No. 4 is a structural austenitic steel based on Fe–Cr–Ni, further MM4 (Fe–Cr–Ni), which is corrosion-resistant and is used for pipeline parts and load-bearing elements operating in aggressive environments. The chemical composition of MM4 (Fe–Cr–Ni) steel is shown in Table 4.

Mechanical tests of plane MM specimens for uniaxial tension were conducted. The preparation and fracture of the specimens were carried out in accordance with GOST 21631–76, GOST 11701–84, and GOST 1497–84, according to which the MM specimens were cut out from the sheet along the rolled product, and the mechanical characteristics of each type of MM were evaluated by four specimens. The geometric characteristics of the specimens are shown in Figure 1.

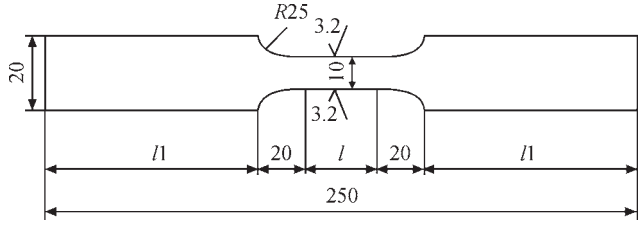

Figure 1. Appearance of specimens for uniaxial tensile tests, where l = 50 mm and $l1$ = 80 mm for grades 5A02 and TA2, l = 40 mm and $l1$ = 90 mm for grades GH3044 and S-06

A visual evaluation of the fracture pattern of the specimens of the four experimental MM was carried out, the results of which are shown in Figure 2, where the specimens δ = 1 mm are shown in Figures 1 and 2 from the top, δ = 3 mm — 3 and 4 from the top.

From the data shown in Figure 2, it can be seen that the specimens of MM1 (Al) alloy were fractured by the expressed shear and tear mechanisms, respectively (Figure 2, *a*), almost without the formation of a "contraction". The specimens of MM2 (Ti) alloy were fractured with the formation of a "contraction" mainly by the tear mechanism (Figure 2, *b*). In this case, small "shear lips" are formed along the edges of the fracture zone. The specimens of MM4 (Fe–Cr–Ni) steel (Figure 2, *c*) and MM3 (Ni) alloy (Figure 2, *d*) were fractured by the expressed shear and tear mechanisms, respectively.

The main mechanical characteristics of MM fracture as a result of static tension are given in Table 5.

The results of the chemical composition data of the aluminium MM1 (Al) alloy (Table 1) indicate that it is close to the AMg2H alloy, and the value of σ_t — to the AMg6 alloy. Titanium MM2 (Ti) alloy and nickel MM3 (Ni) alloy are characterized by high values of δ_y (lines 3–6), that creates prerequisites for the relaxation of RWS in the experimental MM as a result of electrodynamic effects and determines their prospects for the application

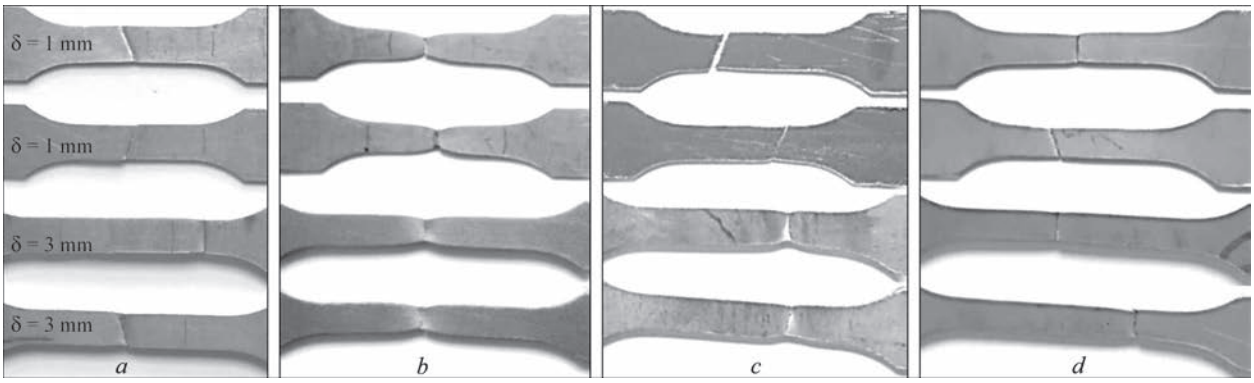

Figure 2. Appearance of fractured specimens δ = 1 and 3 mm: *a* — MM1 alloy (Al); *b* — MM2 alloy (Ti); *c* — MM4 steel (Fe–Cr–Ni); *d* — MM3 alloy (Ni)

Table 6. TIG modes — welding of MM plates δ = 1 and 3 mm

No.	Material	Arc voltage U_a, V	Arc current I_a, A	Welding speed v_w, mm/s	Electrode diameter d_e, mm	Arc gap L_a, mm
1	MM1 (Al)	12.8(13.5)	120(140)	5.0	2.4	2.0
2	MM2 (Ti)	10.2(11.3)	110(130)			1.5
3	MM4 (Fe–Cr–Ni)	11.6(11.9)	140(160)	5.5		
4	MM3 (Ni)	11.0(11.4)	140(160)			
Note. The first value of U_a, I_a — for δ = 1 mm, other — for δ = 3 mm.						

of EDT to them. MM4 (Fe–Cr–Ni) steel is characterized by rather high values of $\sigma_{0.2}$ (lines 7–8).

The formation of RWS in MM butt joint specimens was carried out using TIG welding in Ar. TIG process modes for different grades of MM are presented in Table 6.

As specimens of welded joints, MM plates with dimensions of 500×200 mm and δ = 1 and 3 mm were used, cut out along the rolled product similarly to the specimens for mechanical tests. The TIG process was carried out in a specialized assembly and welding bench (Figure 3), which provided Ar blowing to the welding zone and the cooling weld at laminar gas flow from the torch nozzle at a rate of 12 l/min. The design of the assembly bench provided blowing of the gas environment in the weld root zone due to cavities in the forming lining, through which gas circulated at a flow rate of 2 l/min (Figure 3, *a*). The TIG torch was equipped with a boot-shaped casing that isolated the cooling weld metal from atmospheric oxygen by blowing the outer surface of the welded joint with argon at a flow rate of 10 l/min (Figure 3, *b*). Based on the data in Table 6, a series of welded joint specimens made of MM was produced.

RWS of the specimens were measured by electron speckle-interferometry [18]. The method was selected due to the need to preserve the integrity of the specimen after recording its initial stress state. The specimens with the initial RWS distribution were subjected to EDT, and then the stresses were evaluated again. The effectiveness of EDT was determined by comparing the peak tensile RWS values and their distributions in the central cross-section of the specimens before and after the treatment. The longitudinal (along the weld) σ_x RWS component of the studied MM was evaluated, which has the greatest impact on the service life of welded structures [1].

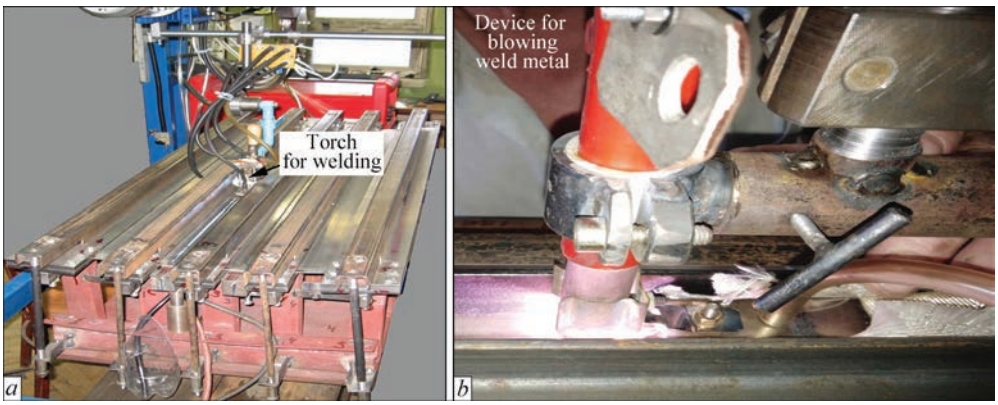

Figure 3. Appearance of the complex for TIG welding of MM: *a* — bench for assembly and welding of specimens; *b* — TIG process using blowing of the outer surface of the cooling weld metal (for TA2 alloy)

EDT PROCESS FOR WELDED JOINTS OF MM

To perform EDT, a hardware complex consisting of a power source and an electrode device (ED) was used. It was previously used for the treatment of aircraft structures [13, 14]. Before EDT, the welded joint specimens were fixed on a rigid base. EDT was performed in a "one direction" with the ED held manually, and the distance between the EDT zones ("EDT pitch") was set in the range of 5–10 mm. The treatment was applied to the outer surface of the weld centre and/or base metal along the fusion lines on both sides of the weld. The areas of the metal surface were treated, where the initial (before EDT) values of tensile σ_x were maximum (where the negative effect of RWS on the mechanical characteristics of the joint is maximum). The EDT conditions and modes for MM specimens are given in Table 7, where the values of the charging voltage and current U_{ch}^{I}, dynamic (impact) U_{ch}^{P} of EDT components and the time period of their action, respectively t_I and t_P.

RESULTS OF EDT ON RWS OF MM SPECIMENS AND THEIR DISCUSSION

The distribution of the RWS σ_x component in the central cross-section of the MM1 (Al) alloy specimen $\delta = 1.0$ mm before and after EDT under the conditions given in Table 7 (line 1) is shown in Figure 4. It can be seen that the treatment has a positive effect on the distribution of σ_x along the fusion lines ($Y = -10$ and 10 mm), where the tensile σ_x values after EDT decrease from 205 to 155 MPa.

The distribution of σ_x RWS in the MM1 (Al) alloy specimen $\delta = 3$ mm before and after EDT under the conditions given in Table 7 (line 2) is shown in Figure 5. It can be seen that after EDT, the initial tensile RWS $\sigma_x = 180$ MPa in the centre of the weld ($Y = 0$) are transformed into compression $\sigma_x = -15$ MPa, and in the base metal along the fusion line ($Y = -5$ and 5 mm), the tensile σ_x values also significantly decrease.

Distribution of the RWS σ_x component in the austenitic MM4 (Fe–Cr–Ni) steel specimen $\delta = 1$ mm before and after EDT under the conditions given in Table 7 (line 3) is shown in Figure 6.

From Figure 6, it can be seen that in the centre of the weld ($Y = 0$), the initial (before EDT) σ_x are compressive, and their values reach –111 MPa. This can be explained by the peculiarity of the structure formation mechanism during the formation of RWS in austenitic steels at rapid cooling of the weld metal. If the structural transformations of the weld metal during cooling occur at low temperatures, its contraction is replaced by a sharp expansion, and the resulting tensile stresses decrease and transfer to compression [19]. The conditions for rapid cooling of the metal were realized during welding of the experimental specimens in the assembly bench (Figure 3, *a*), where inert gas was used to blow the weld. At the same time, in the areas of the base metal near the fusion lines ($Y = -10$ and $Y = 10$ mm), the initial tensile σ_x have the values of 560 and 723 MPa, which after EDT under the conditions of Table 7 (line 3) decrease to 131 and 0 MPa, respectively. At the same time, EDT of the base metal near the fusion line ($Y = -10$ and $Y = 10$ mm) contributes to a decrease in compressive stresses from $\sigma_x = -111$ to –35 MPa in the centre of the weld ($Y = 0$). This can be explained by the redistribution of RWS in the active zone of the welded joint, which is initiated by the relaxation of σ_x near the fusion line.

The EDT of the metal of the MM4 (Fe–Cr–Ni) welded joint specimen $\delta = 3$ mm was performed under the conditions of Table 7 (line 4), taking into account the results obtained for the specimen $\delta = 1$ mm regarding the reduction of compressive stresses in the centre of the weld initiated by the treatment of the fusion lines. EDT was performed along the weld centre and fusion lines. The distribution of RWS σ_x of S-06 steel $\delta = 3$ mm before and after EDT is shown in Figure 7.

From the data in Figure 7, it can be seen that EDT has a positive effect on the distribution of σ_x in the centre of the weld ($Y = 0$). In this zone, the compressive σ_x values grow from –100 to –250 MPa as a result of the EDT. At the same time, EDT also optimizes the distribution of σ_x along the weld metal fusion line ($Y = 10$ and $Y = -10$ mm), where tensile stresses are reduced from 400 to 0–67 MPa. In the areas ($Y = 5$ mm and $Y = -5$ mm), the RWS after EDT transform from tensile to compressive — from 220 to –100 MPa.

The distribution of the σ_x RWS component in the welded joint specimen of MM2 (Ti) alloy $\delta = 1$ mm before and after EDT of the weld metal under the con-

Table 7. Modes and conditions for performing EDT of specimens of welded joints made of MM

№	MM	δ, mm	t_I, μs	t_P, μs	U_{ch}^{P}, V	U_{ch}^{I}, V	Terms of execution of the EDT of MM
1	MM1 (Al)	1.0	275	325	150	300	Along the fusion line (AFL)
2		3.0			300	500	Along the weld centre (AWC)
3	MM4 (Fe–Cr–Ni)	1.0			200	500	AFL
4		3.0			300	500	AFL + AWC
5	MM2 (Ti)	1.0			200	300	AFL
6		3.0			250	500	AWC
7	MM3 (Ni)	1.0			250	300	AWC
8		3.0			300	500	AWC

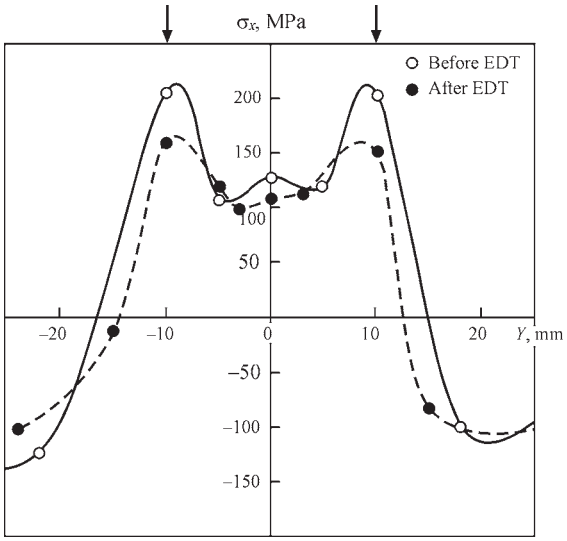

Figure 4. Distribution of the RWS σ_x component in the central cross-section of the MM1 (Al) alloy welded joint specimen δ = 1 mm before and after EDT, where arrows indicate the EDT zones, as in Figures 5–11

ditions of Table 7 (line 5) is shown in Figure 8. It can be seen that EDT reduces the RWS in the centre of the weld (Y = 0) and near the fusion lines (Y = 8 mm and Y = –8 mm), where the values of tensile σ_x after EDT decrease from 200 to 150 MPa and from 270 to 180 MPa, respectively.

The distribution of the RWS σ_x component in the welded joint specimen of MM2 (Ti) alloy δ = 3 mm before and after EDT under the conditions of Table 7 (line 6) of the weld metal is shown in Figure 9. It can be seen that EDT helps to optimize the distribution of RWS in the centre of the weld (Y = 0), where the tensile σ_x after EDT decrease from 200 to 70 MPa. It should be noted that the effect of EDT also extends to σ_x along the fusion line (Y = –8 and Y = 8 mm), where tensile σ_x decrease from 225–240 to 175–180 MPa, respectively.

The distribution of RWS σ_x in the welded joint specimen of nickel MM3 (Ni) alloy δ = 1 mm before

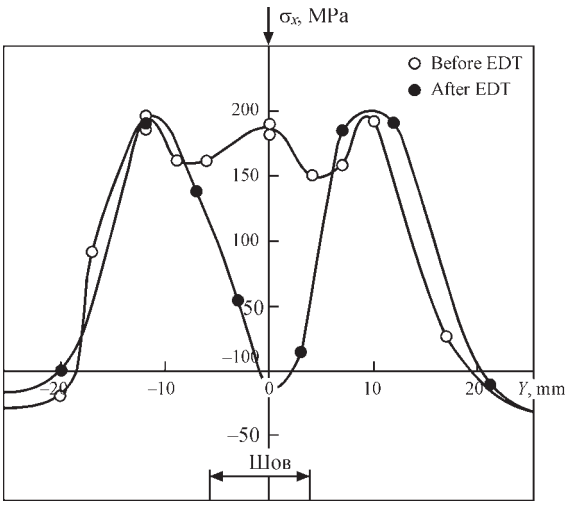

Figure 5. Distribution of the RWS σ_x component in the central cross-section of the MM1 (Al) alloy welded joint specimen δ = 3 mm before and after EDT

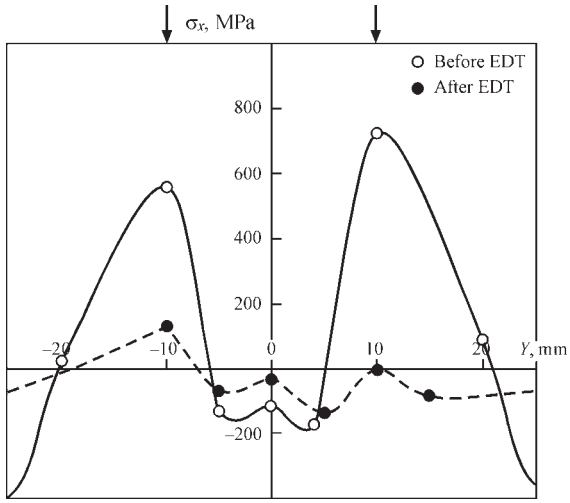

Figure 6. Distribution of the RWS σ_x component in the cross-section of the welded joint specimen made of MM4 (Fe–Cr–Ni) steel δ = 1 mm before and after EDT

and after EDT under the conditions of Table 7 (line 7) is shown in Figure 10, from which it can be concluded that treatment has a significantly lower effect on the distribution of RWS compared to the previous results shown in Figures 4–9. Thus, in the centre of the weld (Y = 0), after EDT, the tensile σ_x decrease from 295 to 263 MPa, and along the fusion lines (Y = –5 and Y = 5 mm) — from 310 to 280 MPa.

The distribution of RWS σ_x in the specimen of MM3 (Ni) alloy δ = 3 mm before and after EDT under the conditions of Table 7 (line 8) is shown in Figure 11. As a result of the studies, it was found that EDT generally has a positive effect on the distribution of RWS in the centre of the weld (Y = 0), where the tensile σ_x after EDT decrease from 305 to 261 MPa.

The summarizing results of evaluating the impact of EDT effectiveness on the control of the RWS σ_x component in the specimens of welded joints made of MM δ = 1 and 3 mm is presented in Table 8. From

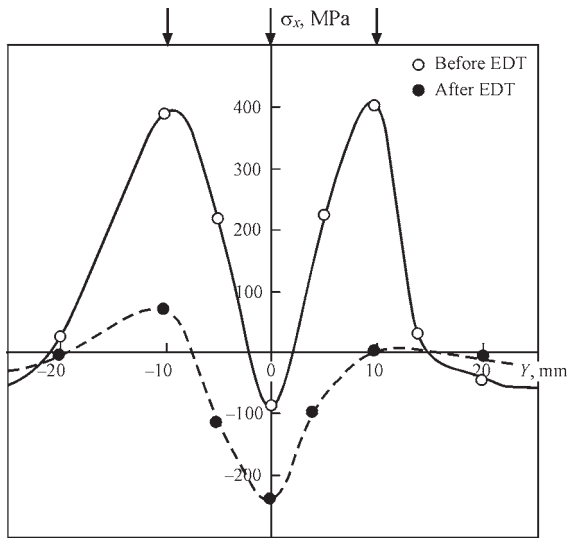

Figure 7. Distribution of RWS σ_x in the cross-section of the welded joint specimen made of MM4 (Fe–Cr–Ni) steel δ = 3 mm before and after EDT

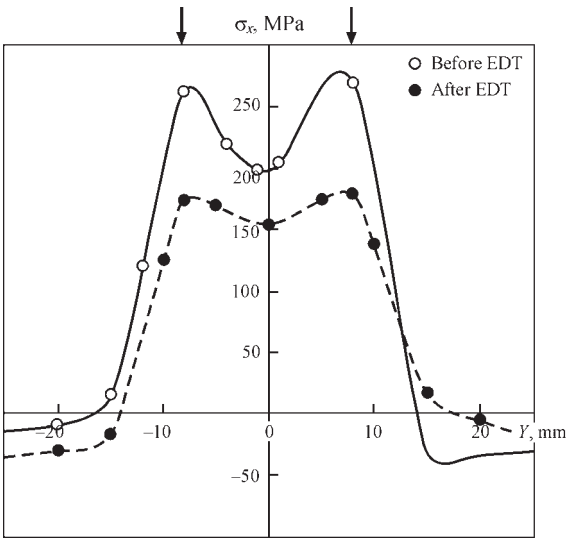

Figure 8. Distribution of the RWS σ_x component in the cross-section of the welded joint specimen of MM2 (Ti) titanium alloy δ = 1 mm before and after EDT

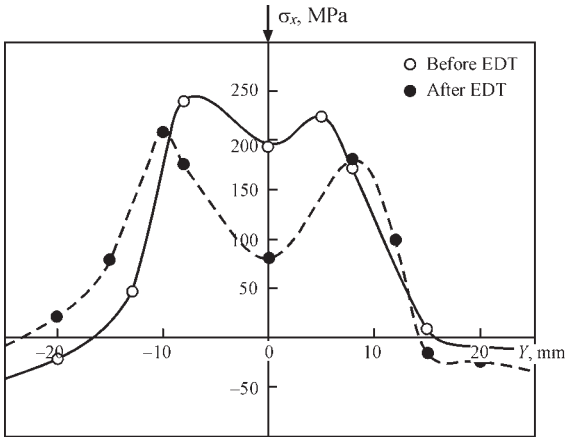

Figure 9. Distribution of the RWS σ_x component in the cross-section of the welded joint specimen of MM2 (Ti) titanium alloy δ = 3 mm before and after EDT

Table 8. EDT effectiveness of welded joints specimens made of MM

No.	MM grade	δ, mm	$\sigma_{x1}^*/\sigma_{x2}$, MPa	$(\sigma_{x1} - \sigma_{x2})/\sigma_{x1}$, %
1	MM1 (Al)	1.0	205/150	30
2		3.0	180/–15	>100
3	MM2 (Ti)	1.0	270/180	35
4		3.0	200/70	65
5	MM4 (Fe–Cr–Ni)	1.0	723/0	100
6		3.0	400/0	100
7	MM3 (Ni)	1.0	295/263	11
8		3.0	305/261	15

*σ_{x1} — maximum values of tensile RWS σ_x before EDT; σ_{x2} — after EDT.

the mentioned results, it can be concluded that EDT is an effective mechanism for the control of the residual stress-strain states of welded joints made of Al and Ti alloys with a thickness of 3 mm (lines 2 and 4, respectively) and austenitic steel (lines 5 and 6). At the same time, optimization of EDT modes within the framework

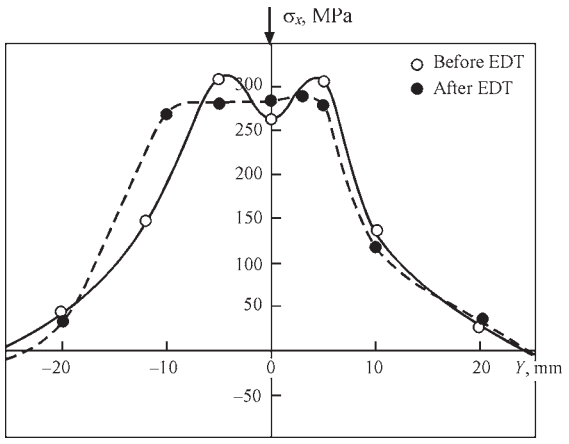

Figure 10. Distribution of the RWS σ_x component in the cross-section of welded joint specimen of nickel MM3 (Ni) alloy δ = 1 mm before and after EDT

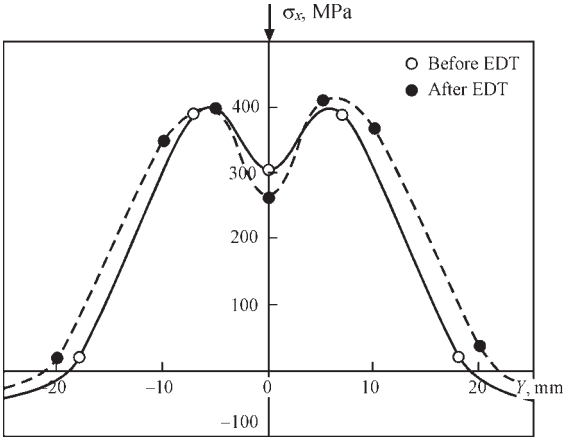

Figure 11. Distribution of the RWS σ_x component in the cross-section of welded joint specimen of MM3 (Ni) alloy δ = 3 mm before and after EDT

of additional studies will increase the effectiveness of the electrodynamic effect for the treatment of welded joints of smaller thicknesses from the supplied materials (with respect to the results presented in lines 1 and 3).

At the same time, the results presented in lines 7 and 8 show that in order to increase the effectiveness of EDT of MM3 (Ni) alloy, it is necessary to use higher values of electrodynamic effect within further studies. It is also advisable to use a new method for the treatment of welded joints made of MM3 (Ni) alloy, based on magnetically pulsed effects on the RWS of welded joints made of non-ferromagnetic MM [2, 3].

Based on the conducted studies, it should be noted that the use of EDT contributes to a reduction in the tensile RWS of thin-sheet welded joints made of the studied MM.

CONCLUSIONS

1. The technology for electrodynamic treatment (EDT) of experimental specimens of thin-sheet butt welded joints made of Al-, Ni- and Ti-based alloys and austenitic steel was developed and implemented.

2. The effect of EDT on the longitudinal σ_x component of residual welding stresses (RWS) of the test specimens was studied using electron speckle interferometry.

3. It was found that EDT provides complete elimination of tensile RWS in welded joints made of Al-based alloy and austenitic steel and reduction in RWS to 65 % from the initial level in Ti-based alloy.

4. It was found that EDT provides a slight decrease in tensile RWS (up to 15 % of the initial level) in welded joints made of Ni-based alloy.

5. Based on the research results, it was found that in order to increase the efficiency of EDT of Ni-based alloy, higher values of electrodynamic action energy or the use of a pulsed magnetic field treatment method are required.

REFERENCES

1. Masubuchi, K. (1980) *Analysis of welded structures*. Oxford, Pergamon Press.
2. Razmyshlyaev, A.D., Ageeva, M.V. (2018) On mechanism of weld metal structure refinement in arc welding under action of magnetic fields (Review). *The Paton Welding J.*, **3**, 25–28. DOI: https://doi.org/10.15407/tpwj2018.03.05
3. Dubodelov, V.I., Goryuk, M.S. (2018) Application of electromagnetic fields and hydrodynamic phenomena to intensify the action on metallic systems: World and Ukrainian experience. In: *Science of Materials: Achievements and Prospects.* Vol. 2, Kyiv, Akademperiodyka, 24–50.
4. Volkogon, V.M., Avramchuk, S.K., Strilets, E.V. (2005) Formation of strengthening coatings under action of powerful electric discharge. In: *Proc. of 5th Int. Sci.-Techn. Conf. on Surface Engineering and Renovation of Products. 21–24 May 2005, Yalta*, 48–51.
5. Conrad, H., Sprecher, A. (1989) *The electroplastic effect in metals*. Ed. by F.R.N. Nabarro. Elsevier Sci. Publs B.V., Dislocations in Solids, 500–529.
6. Baranov, Yu.V., Troitsky, O.A., Avramov, Yu.S. (2001) *Physical principles of electric pulse and electric plastic treatments and new materials.* Moscow, MGIU.
7. Stepanov, G.V., Babutsky, A.I., Mameev, I.A. (2004) Nonstationary stress-strain state in long rod due to the pulse of high density electric current. *Problemy Prochnosti,* **4**, 60–67.
8. Gu, S., Kobayashi, D., Yan et al. (2024) Achieving stress relief in martensitic stainless steel via high-density pulsed electric current treatment. *Metallurgical and Materials Transact. A: Physical Metallurgy and Materials Sci*., 55(**10**), 3859–3868. DOI: https://doi.org/10.1007/s11661-024-07522-5
9. Zhang, X., Xiang, S., Yi, K., Guo, J. (2022) Controlling the residual stress in metallic solids by pulsed electric current. *Acta Metallurgica Sin*. 58(**5**), 581–598, DOI: https://doi.org/10.11900/0412.1961.2021.00367
10. Lobanov, L.M., Pashchin, N.A., Yashchuk, V.A., Mikhodui, O.L. (2015) Effect of electrodynamic treatment on the fracture resistance of the AMg6 aluminum alloy under cyclic loading. *Strength of Materials*, **47**, 447–453. DOI: https://doi.org/10.1007/s11223-015-9676-5
11. Liu, C., Wang, M., Peng, H. et al. (2024) Pulse electric current induced interfacial ductile phase on improving the mechanical properties of the Au20Sn/Cu solder joints. *J. of Materials Sci.: Materials in Electronics*, 35(**18**), 1210. DOI: https://doi.org/10.1007/s10854-024-13002-8
12. Strizhalo, V.A., Novogrudsky, L.S., Vorobiov, E.V. (2008) *Strength of materials at cryogenic temperatures taking into account the action of electromagnetic fields.* Kyiv, IPS.
13. Pashchin, N.A., Zarutsky, A.V. (2016) Influence of electrodynamic treatment of material on fatigue life of specimens with holes. In: *Proc. of Int. Sci.-Techn. Conf. on Problems of Manufacturing and Life Cycle Assurance of Aviation Technique. Kharkiv, 20–21 April 2016* [in Russian].
14. Lobanov, L.M., Pashchin, N.A., Cherkashin, A.V. et al. (2012) Repair welding of intermediate cases of aircraft engines from high-temperature magnesium alloy ML10 with application of electrodynamic treatment. *The Paton Welding J*., **11**, 28–32.
15. Lobanov, L.M., Pashchin, N.A., Loginov, V.P. et al. (2010) Repair of ship hull structures of aluminium alloy AMg6 using electrodynamic treatment. *The Paton Welding J*., **9**, 31–32.
16. Lobanov, L.M., Korzhyk, V.M., Pashchyn, M.O. et al. (2022) Deformation-free TiG welding of AMg6 alloy with application of electrodynamic treatment of weld metal. *The Paton Welding J*., **8**, 3–8. DOI: https://doi.org/10.37434/tpwj2022.08.01
17. Lobanov, L.M., Pashchyn, M.O., Mikhodui, O.L. et al. (2022) Stress-strain state of welded joints of AMg6 alloy after electrodynamic treatment during welding. *Strength of Materials*, 54(**6**), 983–996. DOI: https://doi.org/10.1007/s11223-023-00474-y
18. Lobanov, L.M., Pivtorak, V.A., Savitsky, V.V., Tkachuk, G.I. (2006) Procedure for determination of residual stresses in welded joints and structural elements using electron speckle-interferometry. *The Paton Welding J*., **1**, 24–29.
19. Vinokurov, V.A. (1968) *Welding strains and stresses.* Moscow, Mashinostroenie.

ORCID

L.M. Lobanov: 0000-0001-9296-2335,
M.O. Pashchyn: 0000-0002-2201-5137,
O.L. Mikhodui: 0000-0001-6660-7540

CONFLICT OF INTEREST

The Authors declare no conflict of interest

CORRESPONDING AUTHOR

O.L. Mikhodui
E.O. Paton Electric Welding Institute of the NASU
11 Kazymyr Malevych Str., 03150, Kyiv, Ukraine.
E-mail: olha.mikhodui@gmail.com

SUGGESTED CITATION

L.M. Lobanov, M.O. Pashchyn, O.L. Mikhodui, O.M. Tymoshenko (2025) Electrodynamic treatment for the control of residual stresses in welded joints made of light, heat-resistant alloys and austenitic steel. *The Paton Welding J*., **8**, 37–43.
DOI: https://doi.org/10.37434/tpwj2025.08.04

JOURNAL HOME PAGE

https://patonpublishinghouse.com/eng/journals/tpwj

Received: 15.04.2025
Received in revised form: 19.06.2025
Accepted: 05.08.2025